**International Journal of Mechanical Engineering and Applications**
2022; 10(2): 25-34
http://www.sciencepublishinggroup.com/j/ijmea
doi: 10.11648/j.ijmea.20221002.12
ISSN: 2330-023X (Print); ISSN: 2330-0248 (Online)

# Energy Based Approach to Evaluate Self-Excited Vibrations of Wheelsets Caused by Adhesion Characteristics

**Minyi Yu, Werner Breuer**

Siemens Mobility Rolling Stock Locomotives & Coaches Enigneering Locomotive Sytem Desing Calculation, Siemens Mobility GmbH, Munich, Germany

**Email address:**
minyi.yu@siemens.com (Minyi Yu), werner.breuer@siemens.com (W. Breuer)

**To cite this article:**
Minyi Yu, Werner Breuer. Energy Based Approach to Evaluate Self-Excited Vibrations of Wheelsets Caused by Adhesion Characteristics. *International Journal of Mechanical Engineering and Applications.* Vol. 10, No. 2, 2022, pp. 25-34. doi: 10.11648/j.ijmea.20221002.12

**Received**: March 4, 2022; **Accepted**: April 22, 2022; **Published**: April 28, 2022

**Abstract:** Throughout the homologation process, especially in Germany, the torsional load acting on the wheelset due to drive train oscillations must be evaluated. The maximum values of these dynamic torsional moments are strongly influenced by the adhesion conditions in the wheel/rail contact and the slip velocity range between wheel and rail due to drive control dynamics. The adhesion conditions are hard to measure and to reproduce. Hence, it is time-consuming to prove that the measured dynamic moments cover the possible maximal values. The proposed energy method allows a proper prediction of maximum dynamic moments, assuming critical adhesion conditions and an appropriate drive train model. The criticality of the adhesion conditions is shown by measurements. The method is applied to different types of drive train. The predicted maximum values of the dynamic moments are compared with measurement results. During the drive control design phase, the energy method helps to determine a setting range of the slip velocity compatible with the wheelset axle strength. In the homologation process the method could replace measurements.

**Keywords:** Wheel-Rail Friction, Drive Train, Vibration Analysis, Dynamic Wheel Set Loads

## 1. Introduction

Torsional vibration of powered wheelset axles has become a matter of great interest for rolling stock operation and homologation in recent years due to the observed rotational displacement between axle and wheel interference fits of locomotives [1, 13-16]. When wheels are found to be rotationally displaced, it is assumed that there are dynamic torsional moments occurring that are too high to be transferred by the wheel interference fit. Wheel interference fits can transfer maximum torsional moments of up to 130 kNm, depending on design. Torsional moments of this magnitude can be generated by friction-induced self-excited vibration of the powered wheelset axle: Figure 1 shows a typical measured time history for this. Determining the maximum dynamic torsional moments experimentally is difficult because the adhesion characteristics defined by the frictional contact conditions between wheel and rail play a critical role and cannot easily be reproduced [9, 10]. To estimate the maximum dynamic torsional moment is very important in the design process of the wheelset axle.

These torsional vibrations result from wheel/rail adhesion characteristics that fall off at higher slip velocities in the "macro-slip" zone (Figure 2). Under electric drive or brake torques, the working point of the slip velocity can locate in this zone. Due to negative adhesion coefficient gradient ($\delta\mu/\delta(\Delta v)$) in this zone, the drive train experiences a de-damping effect. If the amount of de-damping is greater than the mechanic damping of drive train, the eigenform with the lowest modal damping in the drive train system starts to vibrate. This is often the torsional eigenform of the wheelset axle, where the two wheels of the wheelset vibrate in phase opposition at the torsional natural frequency of the wheelset axle. This torsional vibration is known as chatter oscillation or torsional oscillation.

The proposed energy method for determining the dynamic torsional moment in wheelset axles makes it possible, assuming conservative frictional conditions, to produce a realistic prediction of the maximum dynamic torsional moment for the entire slip or slip velocity setting range of the drive control system.

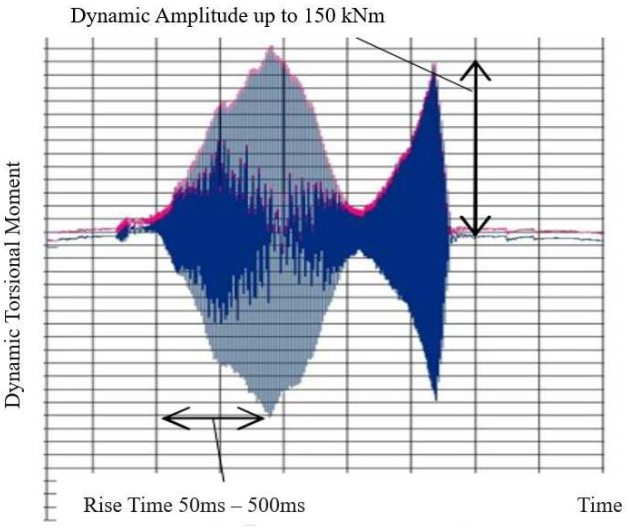


***Figure 1.*** *Example of a dynamic torsional oscillation event in the wheelset axle caused by friction-induced self-excited vibration.*

## 2. Analytical Description of the Dynamic Torsional Moment

Since several decades the theoretical analyses of the torsional oscillation for the drive trains are almost conducted by using numeric simulation in time range and with the objective to reduce the oscillation amplitude if the oscillation occurs, such as in [3-5]. The focus of this article is to evaluate the maximum amplitude of the torsional oscillation with an effective energy-based approach, which is strongly related to the adhesion characteristics between rail and wheel [6].

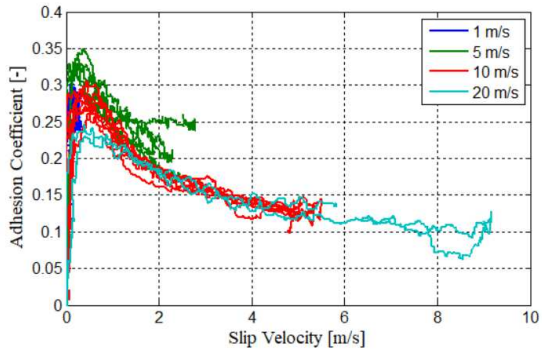


***Figure 2.*** *Wheel/rail adhesion characteristics measured on a Siemens locomotive that could result torsional oscillation of the wheelset axle (the legend is vehicle speed) in [2, 8].*

The de-damping causing the torsional oscillation results from the negative gradient of the wheel/rail adhesion characteristics at higher slip velocities. The degree of de-damping depends on the steepness of the negative gradient at the slip velocity working point or slip working point on the adhesion characteristic curve in the macro-slip zone. With a sufficient de-damping, the torsional oscillation becomes unstable. A limit cycle emerges on the curve of adhesion characteristics. The maximum amplitude is limited for small slips by the stable branch of the adhesion characteristic (micro zone) and by the steady flattening of the adhesion characteristic for large slips. The maximum de-damping is a measure of the criticality of an adhesion characteristic. *Figure 3* summarises these relationships in graphical form.

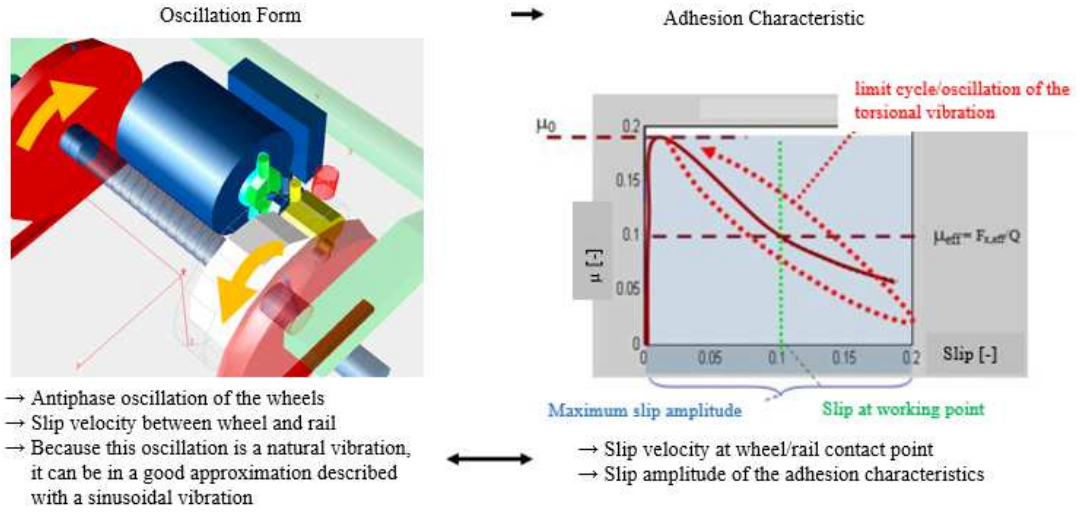


***Figure 3.*** *Relationship between the torsional oscillation and the adhesion characteristic.*

A linear description of the dynamic torsional moment can be derived from the following kinematic relationships:

1. the slip velocity working point $s_0$ gives $\Delta v_{chatter} = s_0 \cdot v$,
2. the sinusoidal oscillation with frequency $f_t$ and $\Delta v_{chatter}$ gives a maximum torsional angle $\Delta\alpha_{chatter,max}$, where $\Delta\alpha_{chatter,max} = \Delta v_{chatter}/(2\,\pi \cdot R \cdot f_t)$ and R is radius of the wheel disc.
3. since wheelset axle damping is low, the maximum torsional moment is given by $M_{t,dyn} = c_{RS} \cdot \Delta\alpha_{chatter,max}$, where $c_{RS}$ is the torsional stiffness,
4. or the linear analytical relationship $M_{t,dyn} = c_{RS} \cdot \Delta v_{chatter}/(2\,\pi \cdot R \cdot f_t)$ applies, the so-called Vogel line.

The relationship defined by the Vogel line gives a conservative estimate of the dynamic torsional moments in the design process.

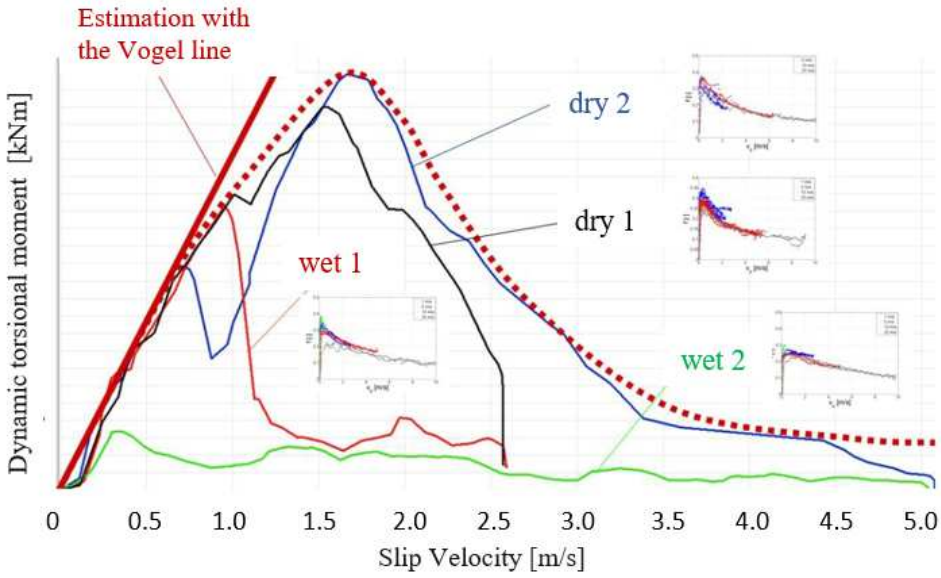


***Figure 4.*** *Dynamic torsional moment as a function of slip velocity between wheel and rail, measured on a Siemens locomotive under four different wheel/rail contact conditions.*

Measurements show that the estimation with the Vogel line applies only for low setting range of slip velocity. The relationship is accordingly as shown in Figure 4:

1. low slip velocity: linear relationship between slip velocity and dynamic torsional moment → Vogel line (example Figure 4: slip velocity up to 0.7 m/s[1]).
2. moderate slip velocity: dynamic torsional moment increases as slip velocity increases, but at a less than linear rate (example Figure 4: slip velocity between 0.7 m/s and 1.7 m/s[1]).
3. high slip velocity: dynamic torsional moment decreases as slip velocity increases (example Figure 4: slip velocity greater than 1.7 m/s[1]).

The estimation with the Vogel line does not take account of the adhesion characteristic and the mechanical damping of the drive train. Hence this estimation leads generally to an overestimation of the dynamic torsional moment for a given slip velocity, especially if it is relatively high.

# 3. Energy Method for Determining the Maximum Dynamic Torsional Moment

The energy method for determining the dynamic torsional moment in wheelset axles is based on the hypothesis that the dynamic torsional moment can be derived from a limit cycle around the relevant slip working point/slip velocity working point. The amplitude of the dynamic torsional moment is determined from the energy balance over this limit cycle.

The proposed algorithm calculates, for any adhesion characteristic, the balance of the elastic energy in the wheelset axle and the energy from the adhesion characteristic that builds up over a limit cycle. The steps necessary to perform this operation are described in the following.

## *3.1. Definition of the Relative Rotational Displacement Angle of the Wheelset Axle as Oscillation Parameter*

Regarding the chatter oscillation, the torsional oscillation of the wheelset system can be described finally with an equivalent single-mass oscillator *(Figure 5)*.

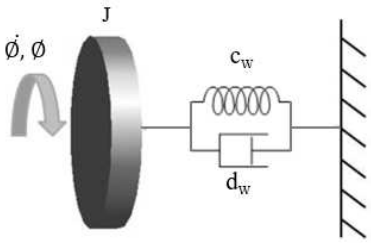


***Figure 5.*** *Equivalent single-mass model of torsional oscillation.*

The angle $\phi$ describes the rotational oscillation angle of the wheelset axle, the relative oscillation angle between the two wheels. In Figure 5, J denotes the resulting moment of inertia of the wheel; the parameters $c_w$ and $d_w$ are the resulting stiffness and damping of the wheelset axle torsional vibration eigenmode. The determination of these parameters is considered in section 4.

The oscillation angle $\phi$ and velocity $\dot{\phi}$ can be described using sine and cosine functions:

$$\phi = A \cdot \sin(\Omega t)\,;\ \dot{\phi} = \mathrm{A} \cdot \Omega \cdot \cos(\Omega t) \qquad (1)$$

where $\Omega = 2\pi f_t$, $f_t$ is the torsional vibration eigenfrequency of the wheelset axle of the drive train and A is the amplitude of the oscillation angle. In design phase the $f_t$ can be calculated by using a simulation model with theoretic drive train parameters. If there are measurements available, $f_t$ can be got directly from these measurements.

1 The given numbers depend on the vehicle and the adhesion characteristic and are therefore not universally applicable.

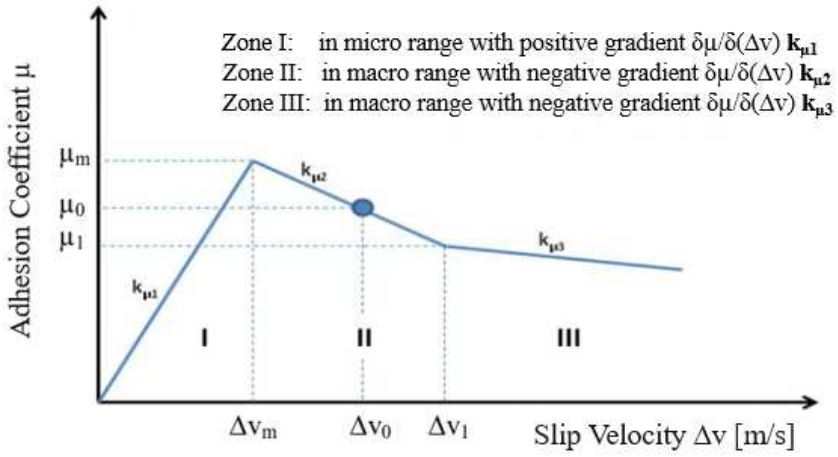


***Figure 6.*** *Adhesion characteristics with three straight lines.*

### *3.2. Adhesion Characteristic as a Function of the Slip Velocity – μ(Δv)*

For sake of clarity, the adhesion characteristic μ(Δv) is shown here only with three straight lines (*Figure 6*). It can be approximated more precisely for practical application. The adhesion characteristic μ(Δv) is expressed in formulae as:

$$\mu(\Delta v) = \begin{cases} \mu_0 + k_{\mu 1} \cdot (\Delta v - \Delta v_m) + k_{\mu 2} \cdot (\Delta v_m - \Delta v_0), \\ \qquad 0 \le \Delta v < \Delta v_m \\ \mu_0 + k_{\mu 2} \cdot (\Delta v - \Delta v_0), \\ \qquad \Delta v_m \le \Delta v < \Delta v_1 \\ u_0 + k_{\mu 3} \cdot (\Delta v - \Delta v_1) + k_{\mu 2} \cdot (\Delta v_1 - \Delta v_0), \\ \qquad \Delta v_1 \le \Delta v < \infty \end{cases} \tag{2}$$

where $\Delta v_0$ is the slip velocity at working point and $\mu_0$ is the adhesion coefficient at $\Delta v_0$. Using the slip velocity definition,

$$\Delta v = \omega \cdot R - v_0 \tag{3}$$

the wheel rotational velocity at the break points in the graph in Figure 6 can be calculated:

$$\omega_m = \frac{\Delta v_m + v_0}{R}; \quad \omega_0 = \frac{\Delta v_0 + v_0}{R}; \quad \omega_1 = \frac{\Delta v_1 + v_0}{R}. \tag{4}$$

In (3), $v_0$ is the running speed, R is the radius of the wheel and ω is the wheel rotational speed.

### *3.3. Dynamic Slip Velocity and Moment $M_{RS}$ at the Wheel as a Function of the Oscillation Speed*

When the torsional oscillation develops, the slip velocity oscillates about the working point $\Delta v_0$. This oscillation can be represented as a function of the oscillation speed:

$$\Delta v(\dot{\phi}) = \Delta v_0 + \dot{\phi} \cdot R \tag{5}$$

This yields the tangential force $F_x = \mu(\Delta v) \cdot Q$, with wheel/rail vertical contact force Q. This force generates the dynamic moment $M_{RS}$ at the wheel. Using the adhesion characteristic according to equation (2), $M_{RS}(\Delta v)$ is:

$$M_{\mathrm{RS}}(\Delta v) = Q \cdot R \cdot \begin{cases} k_{\mu 1} \cdot (\Delta v - \Delta v_m) + k_{\mu 2} \cdot (\Delta v_m - \Delta v_0), \\ \qquad 0 \le \Delta v < \Delta v_m \\ k_{\mu 2} \cdot (\Delta v - \Delta v_0), \\ \qquad \Delta v_m \le \Delta v < \Delta v_1 \\ k_{\mu 3} \cdot (\Delta v - \Delta v_1) + k_{\mu 2} \cdot (\Delta v_1 - \Delta v_0), \\ \qquad \Delta v_1 \le \Delta v < \infty \end{cases} \tag{6}$$

The moment at the wheel can be represented as a function of the oscillation speed $\dot{\phi}$ by using equation (5) in equation (6):

$$M_{\mathrm{RS}}(\Delta v,\dot{\phi}) = Q \cdot R \cdot \begin{cases} k_{\mu 1} \cdot R \cdot \dot{\phi} + (\Delta v_0 - \Delta v_m) \cdot (k_{\mu 1} - k_{\mu 2}), \\ \qquad 0 \le \Delta v < \Delta v_m \\ k_{\mu 2} \cdot R \cdot \dot{\phi}, \\ \qquad \Delta v_m \le \Delta v < \Delta v_1 \\ k_{\mu 3} \cdot R \cdot \dot{\phi} + (\Delta v_1 - \Delta v_0) \cdot (k_{\mu 2} - k_{\mu 3}), \\ \qquad \Delta v_1 \le \Delta v < \infty \end{cases} \tag{7}$$

### *3.4. Sign of the Oscillation Speed ϕ and Transition Points*

Equation (5) can be rearranged to produce the following relationship for the oscillation speed $\dot{\phi}$ as a function of the slip velocity:

$$\dot{\phi} = \frac{\Delta v - \Delta v_0}{R} \tag{8}$$

***Table 1.*** *Value range and sign of the oscillation speed $\dot{\phi}$.*

| | **in zone I** | **in zone II** | **in zone III** |
|---|---|---|---|
| Value range for $\dot{\phi}$ | $\frac{-\Delta v_0}{R} \le \dot{\phi} < \omega_m - \omega_0)$ | $\omega_m - \omega_0 \le \dot{\phi} < \omega_1 - \omega_0$ | $\omega_1 - \omega_0 \le \dot{\phi} < \infty$ |
| Sign for $\dot{\phi}$ | negative | from negative to positive | positive |

***Table 2.*** *Times at which the oscillation cycle switches between zones I, II and III starting from working point $\Delta v_0$, i.e., from $t_0$ to $t_5$ according to Figure 7.*

| Time transition points | t0 | t1 | t2 | t3 | t4 | t5 |
|---|---|---|---|---|---|---|
| Time | 0 | $\frac{1}{\Omega}\sin^{-1}(\frac{\Delta v_1 - \Delta v_0}{A \cdot R})$ | $\frac{\pi}{\Omega} - t_1$ | $\frac{1}{\Omega}(\pi + \sin^{-1}(\frac{\Delta v_0 - \Delta v_m}{A \cdot R})$ | $\frac{3\pi}{\Omega} - t_3$ | $\frac{2\pi}{\Omega}$ |

The sign of the oscillation speed in all slip velocity zones of the adhesion curve can be determined using equation (8) (Figure 7): times $t_0$ to $t_5$ mark the transition points between the slip velocity zones. Times $t_0$ to $t_5$ at which the limit cycle switches between zones I, II and III, starting from working point $s_0$, can be determined with reference to Table 1 and Figure 8. Table 2 summarises the relationships.

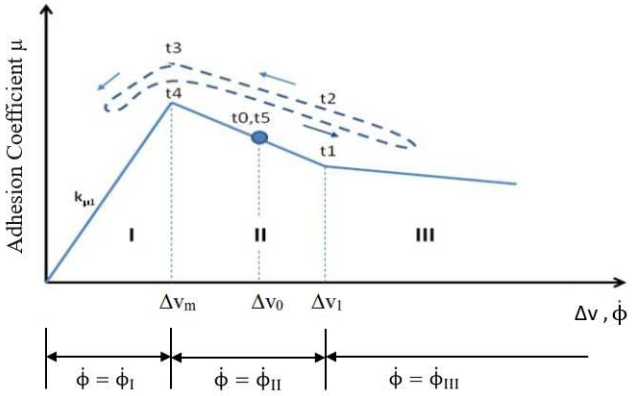


***Figure 7.*** *Slip velocity oscillation during one limit cycle.*

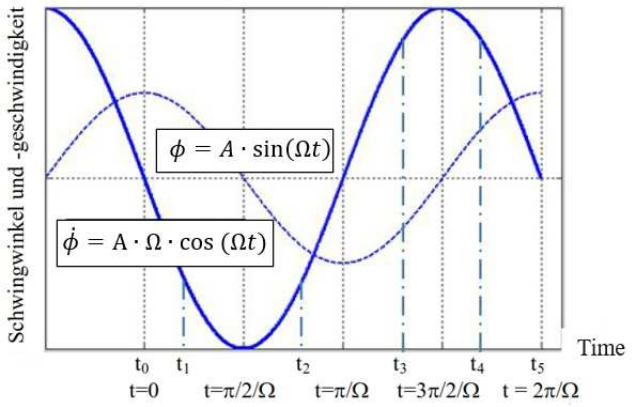


***Figure 8.*** *Time history of the oscillation angle and speed within one oscillation period, $t_0$ to $t_5$ according to Figure 7.*

### *3.5. Energy Balance $E_\mu$ over One Oscillation Period*

The oscillation energy of the slip velocity oscillation $E_{\mu,i}$ in the three zones of the adhesion characteristic is calculated over one oscillation period:

Zone I

$$E_{\mu 1} = Q \cdot R \cdot \int_{t3}^{t4} (k_{\mu 1} \cdot R \cdot \dot{\phi} + c_1) \cdot \dot{\phi} \cdot dt$$

$$= Q \cdot R^2 \cdot k_{\mu 1} A^2 (\frac{t}{2} - \frac{1}{4\Omega} sin(2\Omega t))\Big|_{t3}^{t4} - A \cdot \Omega \cdot c_1 \cdot Q \cdot R \cdot [cos(\Omega t)]\Big|_{t3}^{t4} \quad (9)$$

with $c_1 = (\Delta v_0 - \Delta v_m) \cdot (k_{\mu 1} - k_{\mu 2})$.

Zone II

$$E_{\mu 2} = Q \cdot R \cdot \int_{t0,t2,t4}^{t1,t3,t5} (k_{\mu 2} \cdot \frac{R \cdot \dot{\phi}}{v0}) \cdot \dot{\phi} \cdot dt$$

$$= Q \cdot R^2 \cdot k_{\mu 2} A^2 \cdot (\frac{t}{2} - \frac{1}{4\Omega} sin(2\Omega t))\Big|_{t0,t2,t4}^{t1,t3,t5}. \quad (10)$$

Zone III

$$E_{\mu 3} = Q \cdot R \cdot \int_{t1}^{t2} (k_{\mu 3} \cdot R \cdot \dot{\phi} + d_1) \cdot \dot{\phi} \cdot dt$$

$$= Q \cdot R^2 \cdot k_{\mu 3} A^2 \cdot (\frac{t}{2} - \frac{1}{4\Omega} sin(2\Omega t))\Big|_{t1}^{t2} - A \cdot \Omega \cdot d_1 \cdot Q \cdot R \cdot [cos(\Omega t]\Big|_{t1}^{t2} \quad (11)$$

with $d_1 = (\Delta v_1 - \Delta v_0) \cdot (k_{\mu 2} - k_{\mu 3})$.

This yields the total oscillation energy over one oscillation period $E_\mu$:

$$E_\mu(\Delta v_0, A) = E_{\mu 1}(\Delta v_0, A) + E_{\mu 2}(\Delta v_0, A) + E_{\mu 3}(\Delta v_0, A). \quad (12)$$

The oscillation energy $E_{RS}$ absorbed by the resulting wheelset axle damping is:

$$E_{RS} = d_W \cdot A^2 \cdot \pi \cdot \Omega \quad (13)$$

where A is the amplitude of the oscillation and $d_w$ is the resulting damping of the wheelset. An example representing the curve for the energy components $E_\mu(\Delta v_0, A)$ and $E_{RS}(A)$ for a slip velocity working point $\Delta v_0$ as a function of the oscillation angle amplitude A is shown in Figure 9.

The maximum dynamic torsional moment $M_{t,dyn,max}$ for a slip velocity working point $\Delta v_0$ can be determined as a function of the oscillation angle $A_{max}$ at the point at which the energy $E_{RS}$ absorbed by the resulting wheelset axle damping is equal to the energy $E_\mu$ generated by the adhesion:

$$M_{t,dyn,max}(\Delta v_0) = c_w \, A_{max}(\Delta v_0) \quad (14)$$

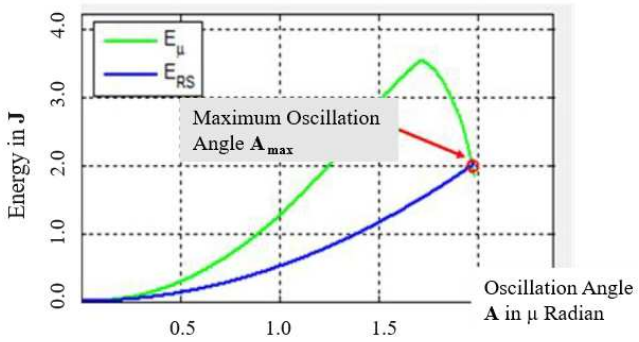


***Figure 9.*** *Energy as function of the oscillation angle amplitude A for a slip velocity working point $\Delta v_0$.*

The oscillation angle amplitude $A_{max}(\Delta v_0)$ for which $E_{RS}(A) = E_\mu(\Delta v_0, A)$ must be determined for each of the considered slip velocity working points $\Delta v_0$. The blue curve in the example presented in Figure 10 shows the curve of the resulting dynamic torsional moment as a function of the slip velocity working point, together with the used adhesion characteristic. The blue curve exhibits three distinct zones.

In zone I, the resulting wheelset energy $E_{RS}$ and the adhesion absorbed energy $E_\mu$ have a point of intersection at 0 for each of the amplitude A of the oscillation angle: the dynamic torsional moment is zero if the working point locates in this zone.

If the working point is in zone II and the amount of de-damping is greater than the resulting damping of the drive train system, it causes the friction-induced self-excited vibration i.e., the chatter oscillation. Once the absorbed energy from the drive train system equals the energy of the de-damping (including in Zone I and III), the maximus oscillation amplitude is reached. The maximum dynamic torsional moment and the section of the adhesion characteristic with the greatest de-damping locate in this zone.

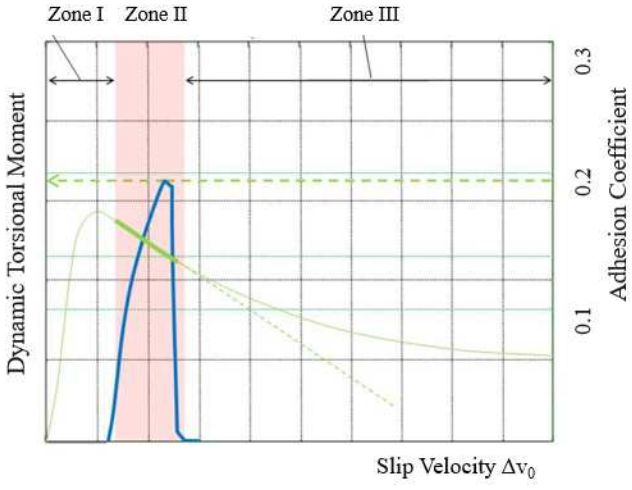


***Figure 10.*** *Dynamic torsional moment as a function of the slip velocity working points (blue curve) and the associated adhesion characteristic (green curve).*

In zone III, the adhesion curve is flat and de-damping is lower than the resulting damping of the wheelset axle. Consequently, the chatter oscillation cannot develop. Due to local scattering of the adhesion characteristic, there can be a marginal chatter oscillation in this zone, but the amplitude of the oscillation cannot develop great. Hence it is impossible, that the dynamic torsional moment establishes a secondary peak in the zone III of higher slip velocity working points: the shape of the adhesion characteristic determines the maximum dynamic torsional moment, and it locates in zone II.

The key parameters applying the energy method are the maximum de-damping of the adhesion characteristic and the drive train damping.

# 4. Significance of the Drive Train Design

Under the mechanism of friction-induced self-excited vibration the drive train will oscillate in the eigenform with the lowest damping. It has hitherto been assumed that this eigenform is the torsional eigenform of the wheelset axle. This assumption must be examined for a specific drive train designs by means of a theoretical or experimental vibration analysis.

The determination of the drive train stiffness and damping parameters is of central importance when applying a theoretical method. *Figure 11* shows a block diagram example of a torsional oscillator model for a partially suspended drive train.

For drive train designs with fully suspended or partially suspended drives, with no relevant dynamic masses between the gear unit and the wheel discs, the torsional wheelset axle stiffness $c_{RS}$ can be calculated from the wheelset axle geometry. If a drive train design with partially suspended or axle suspended drives does have relevant dynamic masses (such as axle-mounted brake discs) between the gear unit and the wheel discs, these dynamic masses must be factored in when determining the resulting axle torsional stiffness $c_{RS}$.

The damping parameters of the drive train elements must be determined with care. It is recommended to check the plausibility of the damping of the individual drive train elements and/or the resulting damping of the drive train eigenforms experimentally.

In the case of partially suspended or axle suspended drive train designs the relevant eigenform is the wheelset axle torsional eigenform, because for these drive train designs this eigenform has the lowest damping.

In the case of fully suspended drive train designs the damping of the torsional eigenforms of the wheelset axle and the hollow shaft must be assessed. If the hollow shaft eigenform exhibits the lowest damping, no torsional oscillation of the wheelset axle occurs.

The energy method describes the wheelset using a single-mass oscillator: the determining parameters are the resulting stiffness $c_w$ and the resulting damping $d_w$. The resulting stiffness $c_w$ is calculated using the frequency $f_t$ of the wheelset axle torsional eigenform:

$$c_w = (2\,\pi\,f_t)^2 \cdot J. \qquad (15)$$

The resulting inertia J is the moment of inertia of the wheel disc. The resulting damping $d_w$ of the single-mass oscillator is equal to the damping of the wheelset axle

torsional eigenform. The additional damping from drive control system shall also be considered (Figure 11).

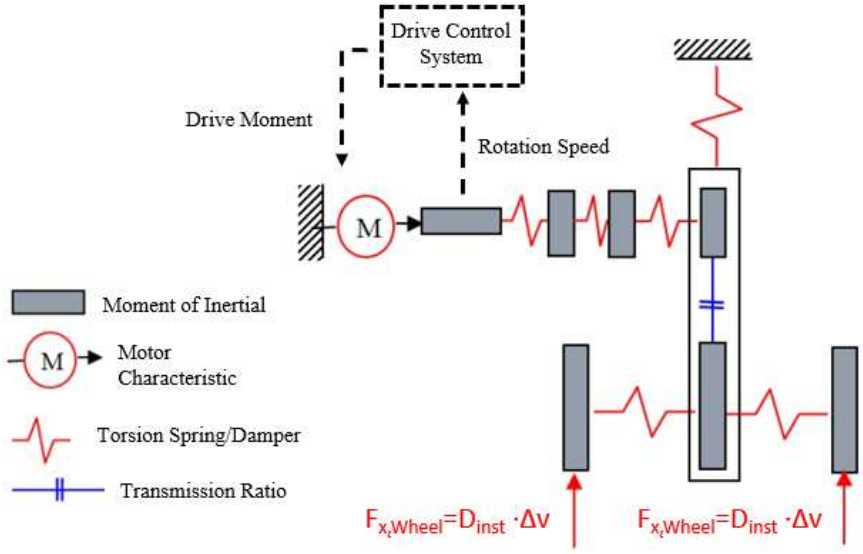


***Figure 11.*** *Block diagram of the torsional vibration model of a typical partially suspended drive train system.*

## 5. Significance of the Frictional Connection Characteristic

*Figure 12* shows how different adhesion characteristics affect the dynamic torsional moment: the green adhesion curve has a high adhesion coefficient $\mu_M$ and low de-damping, the violet adhesion curve has a low adhesion coefficient $\mu_M$ and high de-damping. The maximum dynamic torsional moment is determined by the level of de-damping: despite the lower $\mu_M$ of the violet adhesion curve, the maximum dynamic torsional moment is higher for this characteristic than with the green adhesion curve. This confirms that de-damping is a suitable measure of the criticality of the adhesion curve.

To provide reliable maximum dynamic torsional moments for different vehicles the underlying adhesion characteristic needs to be conservative and must be transferable to different vehicles.

The energy method also assumes that the shape of the adhesion characteristic $\mu(\Delta v)$ does not change during a torsional oscillation event.

The adhesion characteristic used should be determined by measurement. Experience shows that the de-damping degree is determined to a great extent by the intermediate layer between wheel and rail: measurements with a Siemens locomotive found that a slightly moist, granular intermediate layer has the most significant impact, see the measured adhesion characteristics in *Figure 2* or "dry 2" in *Figure 4*. The energy method uses this adhesion characteristic.

*Figure 13* shows its adhesion gradient $\delta\mu/\delta(\Delta v)$, which has a maximum of -0.16 at a slip velocity of 1.8 km/h. For slip velocities of greater than 4 km/h the graph of the gradient is shown as a dashed line, because it has less of an effect on the level of the maximum dynamic torsional moment.

Based on test runs of more than 8000 km with a BR 101 locomotive, M. Weinhardt has performed a statistical analysis with the measured data [7]. Figure 14 shows the adhesion gradient $\delta\mu/\delta(\Delta v)$ determined from this data with different confidence intervals: the maximum $\delta\mu/\delta(\Delta v)$ is -0.18 at a slip velocity of approximately 2 km/h.

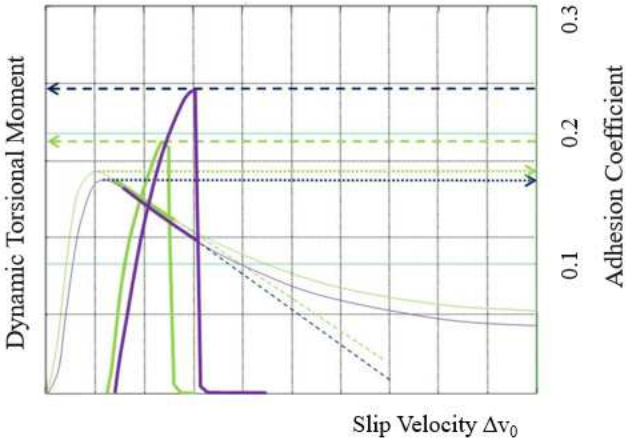


***Figure 12.*** *Comparison of the dynamic torsional moments for different adhesion characteristics as a function of the slip velocity working points – green adhesion–characteristic high $\mu_M$ and low de-damping, blue adhesion characteristic low $\mu_M$ and high de-damping.*

Hence, two investigations using completely different methods deliver very similar results for the maximum adhesion gradient $\delta\mu/\delta(\Delta v)$. This leads the authors to conclude, that the adhesion characteristic used by the energy method is conservative in the slip velocity zone of significance for the determination of the maximum dynamic torsional moment.

Tribological studies show that the adhesion characteristic is determined mainly by the wheel/rail contact configuration [8, 9]: described by the surface roughness of wheel and rail, the presence of an intermediate layer and the compressive load at the contact point.

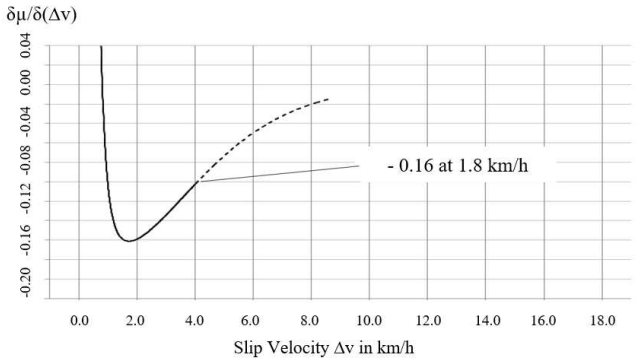


***Figure 13.*** *Adhesion coefficient gradient (δμ/δ(Δv)) of the adhesion characteristic used in the energy method as a function of the slip velocity.*

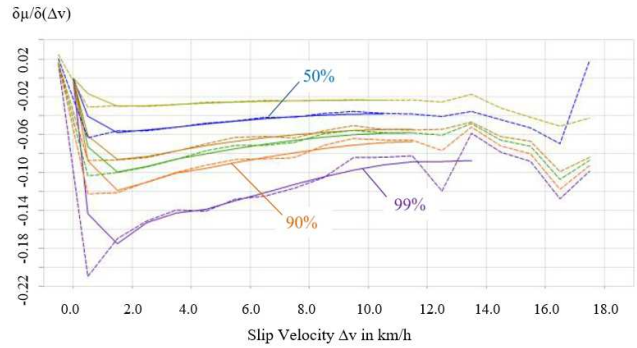


***Figure 14.*** *Adhesion coefficient gradient (δμ/δ(Δv)) determined with the BR 101 as a function of the slip velocity for confidence intervals of 10% to 99% (violet curves) – the negative maximum adhesion coefficient gradient is at approximately -0.18 [7].*

For an individual vehicle the adhesion characteristic is affected by its weight (wheel load) and by its wheel radius (contact ellipse). Hence, an adhesion characteristic $\mu_{Ref}$ measured with a vehicle can be rescaled for other vehicles $\mu_{new}$ based on these two parameters. The energy method uses an approach in which the maximum of the reference adhesion coefficient $\mu_{M,Ref}$ is converted for the wheel load concerned:

$$\mu_{M,neu} = 0.15 + \frac{\mu_{M,Ref}}{1+0.00212\cdot\kappa_2}, \qquad (16)$$

where $\kappa_2$ is a parameter depending on compressive load and material properties [11].

Measurements show that under unfavourable conditions, oscillation events during which the dynamic torsional moment remains constant can persist for several seconds, if the drive control does not intervene and change the slip velocity setpoint. Therefore, the underlying adhesion characteristic can be regarded as quasi-steady in relation to the high frequent torsional oscillation.

The process, which is non-stationary with respect to adhesion characteristic, exists in the transition from an energy balanced adhesion characteristic to another adhesion characteristic with sufficiently high de-damping.

The shape of the adhesion characteristic μ(Δv) during one oscillation period can be regarded as unvarying without limitations.

# 6. Application Examples

*Figures 15 to 18* compare the dynamic torsional moments calculated using the energy method (blue curve) with measurements (brown points) for different vehicles. All calculations are based on the adhesion characteristic with de-damping according to *Figure 13* measured with a Siemens locomotive and discussed in section 5. Scaling for the relevant wheel loads is performed according to equation (16).

None of the vehicles had chatter protection in the drive control system or it was not active during measurement.

The correlation between the torsional moments determined using the energy method and the measured torsional moments is good for all four vehicles: the maximums of the calculated blue curves are slightly above the brown measurement results in all cases.

Differences between measurement results and energy method-based results can be seen at the slip velocities at which the maximum dynamic torsional moments occur. This stems from a certain scatter on the adhesion during the measurement.

The methodology of the energy method is such that there can be no secondary peaks of dynamic moments at high slip velocities, see chapter 3.5. The used adhesion characteristics is proven conservative, see chapter 5. Hence, there is no possibility of a higher dynamic torsional moment than that calculated by the energy method occurring.

It therefore can be ruled out, that relevant dynamic torsional moment occur at high slip velocities during measurements.

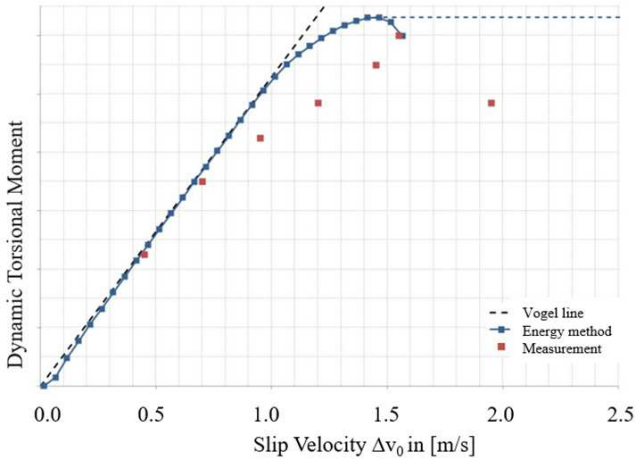


***Figure 15.*** *A vehicle of 90 tonnes with a partially-suspended drive – comparison of dynamic torsional moments from measurement and calculation.*

The effect of the drive train damping on the calculated maximum torsional moment is generally not linear. The amount of effect of non-linearity depends on both the drive train design and the adhesion characteristic: in the application examples, a 20% reduction in drive train damping results in a 30%~60% higher maximum dynamic torsional moment.

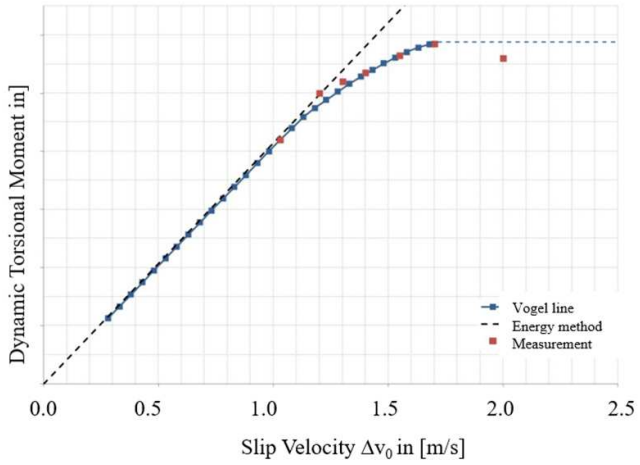


***Figure 16.*** *A vehicle of 86 tonnes with a fully-suspended drive – comparison of dynamic torsional moments from measurement and calculation.*

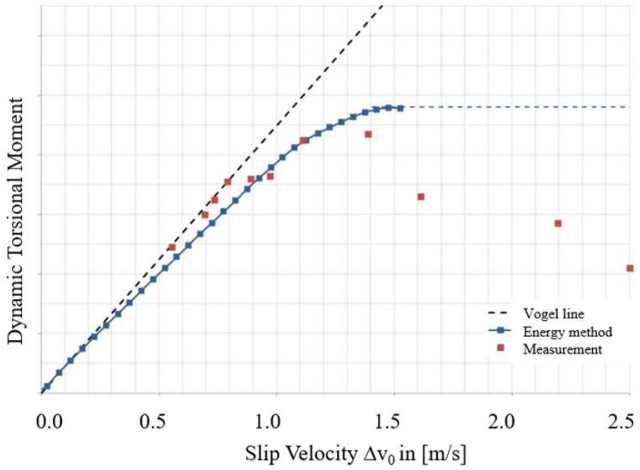


***Figure 17.*** *A vehicle of 70 tonnes with a partially-suspended drive – comparison of dynamic torsional moments from measurement and calculation.*

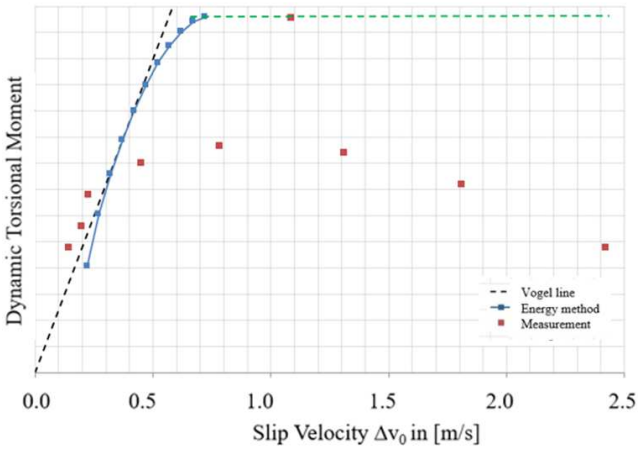


***Figure 18.*** *A vehicle of 54 tonnes with a partially-suspended drive – comparison of dynamic torsional moments from measurement and calculation.*

## 7. Summary

The energy method supplies a reliable estimation of the maximum dynamic torsional moment. The necessary conditions for this are a conservative adhesion characteristic and a sufficiently precise knowledge of the drive train damping. The effect of chatter oscillation protection in drive control system is not considered. The fundamental suitability of the method has been confirmed by an independent commentary [12]. The adhesion characteristic used can be regarded as conservative according to the current state of knowledge because its course through the zone of maximum de-damping has been confirmed by an independent another investigation [7]. The energy method allows to predict the maximum torsional moments of widely differing vehicles. The individual vehicles are covered by the sensitivity of the method to the degree of de-damping and the drive train damping value. The rescaling of the adhesion characteristic for different wheel loads affects the degree of de-damping. These two parameters and the rescaling step have been verified in several instances.

The authors therefore believe that the energy method should be trialled on the widest possible range of vehicles for which dependable measurements are available. This will help to enhance the plausibility of the critical parameters. It would be particularly useful to derive adhesion characteristics from measurements with other vehicles to provide broader verification of the rescaling methodology.

This effort is worth it as the energy method has a significant potential for application. It can be of assistance with the design of the drive control system when specifying the setting range of the slip velocity in drive control system. In the homologation process the energy method could render measurements unnecessary for the provision of proof for vehicles with no chatter or rolling vibration protection. Measurement investigations of the maximum torsional moment are currently mandatory for verification of wheelset torsional oscillation in Germany [13].

The authors are aware that the realization of this potential depends on the general acceptance of the energy method and hope that this article will stimulate the necessary discussion.

## References

[1] Benker, T., Weber, T.: Torsionsschwingungen von Radsaetzen – eine Herausforderung? [Torsional vibrations of wheelsets – challenge?]; EI – Der Eisenbahningenieur [The Railway Engineer], April 2015.

[2] K. Six, A. Meierhofer, G. Mueller, P. Dietmaier: Physical processes in wheel-rail contact and its implications on vehicle-track interaction, Vehicle System Dynamics 53 (5), May 2015.

[3] W. Rulka, W. Breuer, M. Yu, T, Weigel: Echtzeitsimulation der Fahrdynamik Schienenfahrzeugen zur Inbetriebnahme der Fahrzeugsoftware im Labor – HiL [Realtime simulation of the driving dynamics for homologation of the vehicle software in laboratory – HiL], 13. Internationaler Kongress „Berechnung und Simulation im Fahrzeugbau“, VDI Fahrzeug und Verkehrstechnik, September 2006.

[4] M. Fleischer: PhD thesis: Traction Control for Railway Vehicles, Aachener Beitraege Des ISEA, Vol. 128, June 2019.

[5] F. Trimpe, S. Lueck, R. Naumann, C. Salander: Simulation of torsional vibration of driven railway wheelsets respecting the drive control response on the vibration excitation in the wheel-rail contact point, Vibration 4 (2021), pp. 30-48.

[6] M. Yu, W. Breuer: Energie-Methode zur Vorhersage von kraftschlussinduzierten Eigenschwingungen von Radsatzwellen [Energy Method to forecast of self-excited wheelset vibration], 16. Internationale Schienenfahrzeugtagung Dresden, September 2018.

[7] *M. Weinhardt.:* Torsionsschwingung von Radsätzen – Fakten und Thesen zur Anregung durch den Rad/Schiene-Kraftschluss [Torsional vibration of wheelsets – Facts and hypotheses concerning excitation by the wheel/rail frictional connection]; Bombardier Transportation.

[8] 15th International Rail Vehicle Conference Dresden 2017, Conference part 1.

[9] K. Six, C. Tomberger, A. Meierhofer, M. Rosenberger: Tribological processes in the contact between wheel and rail, Tribologie und Schmierungstechnik [Tribology and Lubrication Technology] 59 (5), 44-47, September 2012.

[10] A. Meierhofer: PhD thesis: A new Wheel-Rail Creep Force Model based on Elasto-Plastic Third Body Layers.

[11] *Popov, V. et al:* Friction coefficient in “rail-wheel”-contacts as a function of material and loading parameters; Physical Mesomechanics 53 (2002) 17-24. Elsevier 2015.

[12] *Popov, V.:* Stellungnahme zum Verfahren: Energie-Methode zur Beurteilung von kraftschlussinduzierten Eigenschwingungen von Radsatzwellen [Commentary regarding the technique: energy method for assessing frictional-connection-induced natural vibration of wheelset axles]; Berlin, December 12, 2016.

[13] VDB-Schrift 003: Anforderungen an die Nachweise zu Radsatz-Torsions-schwingungen [Requirements for verification of wheelset torsional vibrations]. Verband der Bahnindustrie Deutschland (VDB) e. V., Berlin 2021; ISBN 978-3-00-068568-2.

[14] *Starlinger, A.:* Langzeitmessung von Rolliermomenten [Longterm Measurements of torsional wheelset moments]; 14th International Rail Vehicle Conference Dresden 2015.

[15] Schneider, R.: Rollierschwingungen – Integrierter und systematischer Ansatz [Torsional wheelset moments – integrated ans systematic approach]; 14th International Rail Vehicle Conference Dresden 2015.

[16] Saur, F.; Weber, J.: Auslegung von Radsatzwellen unter Berücksichtigung des maximalen Torsionsmomentes [Design of wheelset-shafts considering the maximum dynamic torsional moment]; ETR No. 10; October 2010.